

Metastasis-Associated Protein 3 (MTA3) Regulates G2/M Progression in Proliferating Mouse Granulosa Cells¹

Jakub Kwintkiewicz,³ Elizabeth Padilla-Banks,³ Wendy N. Jefferson,³ Ilana M. Jacobs,³ Paul A. Wade,⁴ and Carmen J. Williams^{2,3}

³Reproductive Medicine Group, Laboratory of Reproductive and Developmental Toxicology, National Institute of Environmental Health Sciences, National Institutes of Health, Research Triangle Park, North Carolina

⁴Eukaryotic Transcriptional Regulation Group, Laboratory of Molecular Carcinogenesis, National Institute of Environmental Health Sciences, National Institutes of Health, Research Triangle Park, North Carolina

ABSTRACT

Metastasis-associated protein 3 (MTA3) is a constituent of the Mi-2/nucleosome remodeling and deacetylase (NuRD) protein complex that regulates gene expression by altering chromatin structure and can facilitate cohesin loading onto DNA. The biological function of MTA3 within the NuRD complex is unknown. Herein, we show that MTA3 was expressed highly in granulosa cell nuclei of all ovarian follicle stages and at lower levels in corpora lutea. We tested the hypothesis that MTA3-NuRD complex function is required for granulosa cell proliferation. In the ovary, MTA3 interacted with NuRD proteins CHD4 and HDAC1 and the core cohesin complex protein RAD21. In cultured mouse primary granulosa cells, depletion of endogenous MTA3 using RNA interference slowed cell proliferation; this effect was rescued by coexpression of exogenous MTA3. Slowing of cell proliferation correlated with a significant decrease in cyclin B1 and cyclin B2 expression. Granulosa cell populations lacking MTA3 contained a significantly higher percentage of cells in G2/M phase and a lower percentage in S phase compared with control cells. Furthermore, MTA3 depletion slowed entry into M phase as indicated by reduced phosphorylation of histone H3 at serine 10. These findings provide the first evidence to date that MTA3 interacts with NuRD and cohesin complex proteins in the ovary *in vivo* and regulates G2/M progression in proliferating granulosa cells.

cell cycle, chromatin, cohesin, granulosa cells, NuRD complex, ovary

INTRODUCTION

Ovarian granulosa cells surround an oocyte and together with theca-interstitial cells comprise an endocrine syncytium that provides morphological and biochemical support for ovarian follicle development. Follicle cell proliferation and steroid hormone biosynthesis, rigorously controlled by pituitary hormones and autocrine/paracrine growth factors, are

prerequisites for development of a healthy follicle and ovulation of a developmentally competent oocyte [1–3]. Follicle growth is a carefully orchestrated developmental process controlled by a tightly regulated program of gene expression driven by multiple transcription factors [4].

Dynamic alterations in chromatin structure affect DNA accessibility to the transcriptional apparatus and serve as a mechanism for regulating gene expression [5]. Chromatin structure is altered by repositioning nucleosomes along DNA and by covalent histone or DNA modifications, such as acetylation or methylation. Several chromatin-modifying multi-protein complexes have been identified that are composed of different combinations of subunits that have DNA-binding, DNA helicase, and histone-modifying activities. Chromatin-modifying complexes containing histone acetyltransferases are typically associated with open transcriptionally active chromatin, whereas complexes containing histone deacetylases (HDACs) are associated with densely packed transcriptionally inactive chromatin. In addition, some transcription factors recruit HDACs to chromatin and can act as histone modifiers themselves [6–9].

Chromatin remodeling is important in regulating gene expression responsible for controlling the steroidogenic activity of luteinized granulosa cells [10, 11]. SNF2L, official symbol SMARCA1, the ATP-dependent helicase subunit of the imitation switch (ISWI) chromatin-remodeling complex, is highly upregulated in granulosa cells in response to the luteinizing hormone surge [10]. SMARCA1 becomes associated with the steroidogenic acute regulatory protein (STAR) promoter and induces expression of this critical gene during luteinization. In addition, association of specific transcription factors with the STAR promoter has been linked with alterations in histone modifications [12]. These findings suggest that chromatin modifications are necessary for direct action of transcription factors on gene promoters regulating granulosa cell luteinization.

The Mi-2/nucleosome remodeling and deacetylase (NuRD) protein complex is a chromatin remodeling complex reported to function as a transcription repressor [13, 14]. The NuRD complex contains an ATP-dependent chromodomain helicase DNA-binding protein (CHD3 or CHD4) that provides nucleosome-remodeling activity and either HDAC1 or HDAC2 that provides HDAC activity [15–17]. Additional NuRD subunits include methyl-CpG-binding domain (MBD) proteins, retinoblastoma-associated binding proteins, and metastasis-associated (MTA) proteins. Combinatorial assembly of these subunits into the NuRD complex occurs variably depending on species and cell type and can result in distinct functions [5, 13]. In addition to its chromatin-modifying activities, the NuRD complex was shown in HeLa cells to facilitate association of

¹Supported by grants Z01-ES102985, and Z01-ES101965 from the National Institute of Environmental Health Sciences, Intramural Research Program of the National Institutes of Health.

²Correspondence: Carmen J. Williams, Reproductive Medicine Group, Laboratory of Reproductive and Developmental Toxicology, National Institute of Environmental Health Sciences, National Institutes of Health, P.O. Box 12233, MD E4-05, Research Triangle Park, NC 27709. E-mail: williamsc5@niehs.nih.gov

Received: 26 August 2011.
First decision: 18 September 2011.
Accepted: 25 October 2011.

© 2012 by the Society for the Study of Reproduction, Inc.
eISSN: 1529-7268 <http://www.biolreprod.org>
ISSN: 0006-3363

cohesin with chromosomes [18]. This function could be important in gene regulation because of recent reports that cohesin binding regulates three-dimensional chromosome architecture to bring enhancer and promoter sequences together [19]. The NuRD complex also participates with cohesin in the cellular response to DNA damage, perhaps by affecting cell cycle checkpoints [20–24].

In breast cancer cells, MTA3 expression is positively regulated by estradiol, and the MTA3-NuRD complex supports maintenance of epithelial differentiation [25, 26]. Although these findings connect MTA3 expression with hormonal signaling and cell differentiation in breast tumors, little is known about whether this relationship is conserved in normal female reproductive tissues that are tightly regulated by hormonal signaling. In the present study, we show that MTA3 is highly expressed in granulosa cells of ovarian follicles at all stages of follicular development and that it interacts with NuRD and cohesin complex components in the ovary. Depletion of MTA3 from granulosa cells results in reduction of cyclin B expression and slowing of cell proliferation at the G2/M transition. These findings suggest a functional role for MTA3 in supporting granulosa cell proliferation, possibly via interactions with NuRD and cohesin complex proteins.

MATERIALS AND METHODS

Animals, Tissue Collection, and Cell Culture

CD1 mice were obtained from the in-house breeding colony at the National Institute of Environmental Health Sciences (NIEHS). All animal procedures were performed under an approved NIEHS protocol and were consistent with the Guide for Care and Use of Laboratory Animals. For immunohistochemical analysis, ovarian tissue was collected from mouse pups on Postnatal Days 1–19. To obtain granulosa cells for MTA3 splice variant analysis, adult (6- to 8-wk-old) mice were superovulated using a single injection of 5 IU of equine chorionic gonadotropin (Calbiochem), and pure populations of granulosa cells were collected by mechanical separation of cumulus-oocyte complexes. For granulosa cell culture, ovaries were collected from unstimulated mice on Postnatal Day 20, and cells were obtained by puncturing whole ovaries with a 30G needle in Dulbecco modified Eagle medium-Ham F-12 medium (DMEM/F-12) (1:1; Invitrogen). Cells were then collected by brief centrifugation at 200 × *g*, and viability was determined by trypan blue exclusion. Granulosa cells were seeded (10⁵ cells/well) into 12-well plates (Corning) and cultured in DMEM/F-12 (1:1) in the presence of 10% fetal bovine serum (Hyclone) and media supplements. Cells were washed twice with culture medium 6 h after plating, and then treatments (viral infection) were applied.

Immunohistochemistry

Reproductive tract tissues were fixed in cold formalin for 24 h, embedded in paraffin, and cut at 6 μm. For antigen retrieval, slides were treated with citrate buffer (pH 6.0; Biocare Medical) and then placed in decloaker solution (Biocare Medical). Endogenous peroxidase was quenched with 3% H₂O₂. Tissues were blocked with 10% bovine serum albumin (BSA) and incubated with affinity-purified rabbit polyclonal MTA3 antibody (3.75 μg/ml) [25] in 1× automation buffer (AB) (Biomedica Corp.) containing 1% BSA and 1% milk. Slides were rinsed and incubated with 3 μg/ml of biotinylated anti-rabbit IgG (Vector Laboratories) in AB for 30 min, followed by incubation for 30 min in ExtrAvidin peroxidase (Sigma) diluted 1:50 in AB. Protein was visualized using NOVAREd (Vector Laboratories).

Immunoprecipitation

For immunoprecipitation of MTA3 and CHD4, ovaries from 20-day-old mice were homogenized in immunoprecipitation (IP) lysis buffer (25 mM Tris-HCl, pH 7.4, 150 mM NaCl, 1 mM edetic acid [EDTA], 1% NP-40, and 5% glycerol). For RAD21 immunoprecipitation, ovarian nuclear extracts were obtained in a two-step isolation process using cytosolic (50 mM Tris-HCl, pH 7.4, 1% NP-40, 0.25% deoxycholic acid, and 1 mM EDTA) and nuclear (1% sodium dodecyl sulfate, 50 mM Tris-HCl, pH 8.1, and 10 mM EDTA) extraction buffers. Protein concentration was determined using the BCA protein assay (Pierce). A total of 1000 μg of total protein (MTA3 and CHD4) or 50 μg

of nuclear protein (RAD21) was brought to a 600-μl volume with IP lysis buffer and precleared with 40 μl of a 50% slurry of agarose beads (Pierce). Samples were incubated overnight at 4°C with either rabbit IgG (Santa Cruz), CHD4 (Abcam), MTA3, or RAD21 (Cell Signaling) antibodies at 1.5 mg of antibody per milligram of input protein. Immune complexes were captured by incubation with protein A/protein G agarose resin and eluted using an immunoprecipitation kit (Pierce) following the manufacturer's instructions.

Immunoblotting

Total protein was isolated from cultured granulosa cells or from postnatal ovaries using tissue protein extraction reagent (T-PER; Pierce). For cellular fractionation, we used nuclear, cytoplasmic, and membrane protein extraction reagents (Pierce) following the manufacturer's instructions. Protein content was determined using the BCA protein assay. Protein extracts (50 μg/lane for γH2AX and 10 μg/lane for all other tested proteins) were separated on 4%–12% Tris-glycine minigels and transferred to polyvinylidene fluoride membrane (Invitrogen). Blots were incubated with antibodies at the following concentrations: MTA3 (0.375 μg/ml), cyclin B1 (0.025 μg/ml; Cell Signaling), γH2AX (0.025 μg/ml; Cell Signaling), Trp53 (0.2 μg/ml; Santa Cruz), CHD4 (0.375 μg/ml; Abcam), HDAC1 (0.2 μg/ml; Santa Cruz), or RAD21 (0.075 μg/ml; Cell Signaling). To check protein loading, immunoblots were stripped and reprobed using either actin (Santa Cruz) or glyceraldehyde phosphate dehydrogenase (GAPDH) (Abcam) antibodies. Following extensive washes with Tris-buffered saline with Tween 20, either a horseradish peroxidase-conjugated secondary anti-rabbit IgG (Amersham), anti-mouse IgG (Abcam), or anti-goat IgG (Jackson ImmunoResearch) was applied. Signals were visualized using Pierce Femto or Pico reagents and exposure to film.

RNA Isolation and RT-PCR

Total RNA was isolated from granulosa cells using either a PicoPure RNA isolation kit (Arcturus) or TRIzol reagent (Invitrogen). Reverse transcription was performed using SuperScript first-strand synthesis system (Invitrogen). To determine which MTA3 splice forms were present in granulosa cells, primers were designed based on sequences of the four splice main forms found in the University of California Santa Cruz (UCSC) genome browser (<http://genome.ucsc.edu/>). The PCR was carried out as follows: 5 min at 95°C, then 30 cycles of 95°C for 30 sec, 58°C for 30 sec, and 72°C for 60 sec. The PCR products were resolved using a 1% agarose gel and visualized using a BioSpectrum imaging system (UVP). Real-time PCR with detection by differentially labeled TaqMan minor groove binding probes (TaqMan PCR; Applied Biosystems) was used to determine the ratio of MTA3 sequences containing a three-nucleotide insertion in exon 12. Standard real-time PCR to test expression of various genes relative to ribosomal protein L19 (*Rpl19*) was performed using gene-specific primers and Power SYBR Green Master Mix (ABI). Relative expression was calculated using the delta-delta cycle threshold method [27]. Real-time and TaqMan PCR was carried out using an ABI Prism 7200 sequence detection system. The primers and probes used for all analyses are listed in Supplemental Table S1 (available online at www.biolreprod.org).

Lentivirus Production and Cell Infection

Plasmid pLKO.1 carrying either a scrambled or *Mta3*-specific short hairpin RNA (shRNA) sequence was purchased from Sigma. The sequence of *Mta3*-specific shRNA was as follows: 5'-CCGGCGCAAGATTTCAACGA CATCTCGAGATGTCGTTGAAATCTTTGCCGTTTTTG-3'. The lentivirus was packaged and titered as previously described [28]. Multiplicity of infection was expressed in transducible units per cell (TU/cell) and calculated based on the number of viable granulosa cells plated. Viral particles were added to the cell culture 6 h after seeding.

Cloning and Mutagenesis

Granulosa cell-derived MTA3 variants 1A and 1B cDNA was tagged at the N-terminus by PCR amplification using a primer containing a 2× FLAG sequence. The FLAG-tagged sequences were cloned into the *Bam*HI and *Xho*I sites of pEYFP-N1 (Clontech) to add enhanced yellow fluorescent protein (EYFP) at the C-terminus. The FLAG-tagged and FLAG/EYFP-tagged sequences were inserted by recombination into destination viral vector pDest-673 (generously provided by Dr. Dominic Esposito of the National Cancer Institute). An RNA interference-resistant mutant of the 2× FLAG/MTA3 sequence was generated using the QuikChange Lightning Site-Directed mutagenesis kit (Stratagene). Primers were designed to create a mismatch in the region of *Mta3* mRNA targeted by the *Mta3*-specific shRNA, while at the

same time keeping the amino acid sequence unchanged. The sequences of all primers used for cloning are provided in Supplemental Table S1.

Cell Proliferation Assay

Cell proliferation was measured 24, 48, 72, and 96 h after lentiviral infection using an MTS cell proliferation assay (Promega). Briefly, 20 μ l of staining solution was added to cells at the end of treatment. After incubation for 1–4 h, absorbance at 490 nm was measured.

Immunofluorescence and Confocal Microscopy

Granulosa cells were seeded (10^5 cells/well) in glass-bottom 12-well plates (MatTek) and infected with lentivirus carrying MTA3-EYFP. After 96 h, 5 μ M DRAQ5 (Biostatus Limited) was added to stain DNA. Confocal images were recorded using a Zeiss LSM 510-UV META microscope and processed using Photoshop software (Adobe).

Flow Cytometry

Granulosa cells were collected 96 h after lentiviral infection, fixed in 70% ethanol, permeabilized in 0.2% Triton X-100, and incubated with mouse anti-phospho-histone H3 antibody (10 μ g/ml; Cell Signaling) for 2 h. The secondary antibody was fluorescein isothiocyanate-conjugated anti-mouse IgG (12 μ g/ml; Jackson ImmunoResearch). DNA was stained with 3 μ g/ml of propidium iodide (PI). Flow cytometric analysis was carried out using an FACSsort flow cytometer equipped with CELLQuest software (Becton Dickinson Immunocytometry Systems). Individual cells (7500 per experimental sample) were selected by gating on a PI area vs. width dot plot to exclude cell aggregates and debris. Cell cycle analysis was performed using ModFit software (Verity Software House).

Statistical Analysis

Statistical analyses were performed using Prism software (GraphPad Software, Inc.). The statistical tests used are indicated in the corresponding figure legends.

RESULTS

Expression and Cellular Localization of MTA3 During Follicle Development

To gain new insights into the role of chromatin remodeling during ovarian follicle development, expression of the NuRD component MTA3 was examined in mouse ovaries. MTA3 was expressed in maturing follicles at all stages of postnatal development as indicated by immunohistochemical analysis (Fig. 1A). In the somatic cell compartment, intense positive staining was observed in granulosa cells of all follicle stages (primordial through preovulatory). There was some staining in theca-interstitial and corpus luteum cells, but the signal was much weaker than in granulosa cells. MTA3 staining in all somatic cell types was most intense in the nuclei, although some cytoplasmic signal was also observed. MTA3 was also expressed in developing oocytes at all stages, from primordial to fully grown. Expression of MTA3 in the ovary increased with postnatal age as indicated by immunoblotting (Fig. 1B). To determine if MTA3 expression was induced by gonadotropin stimulation, real-time PCR was performed on ovary cDNA from unstimulated adults and adults treated 48 h previously with equine chorionic gonadotropin. There was no difference in the relative expression of MTA3 after gonadotropin stimulation (data not shown).

To confirm the apparent nuclear localization, granulosa cell extracts were separated into membrane, cytoplasm, and nuclear fractions. Immunoblotting of these fractions indicated that the vast majority of MTA3 localizes to the nuclear compartment (Fig. 1C). Of note, a second immunoreactive band that migrated slightly slower than the predominant MTA3 band was consistently observed in immunoblots of ovary protein,

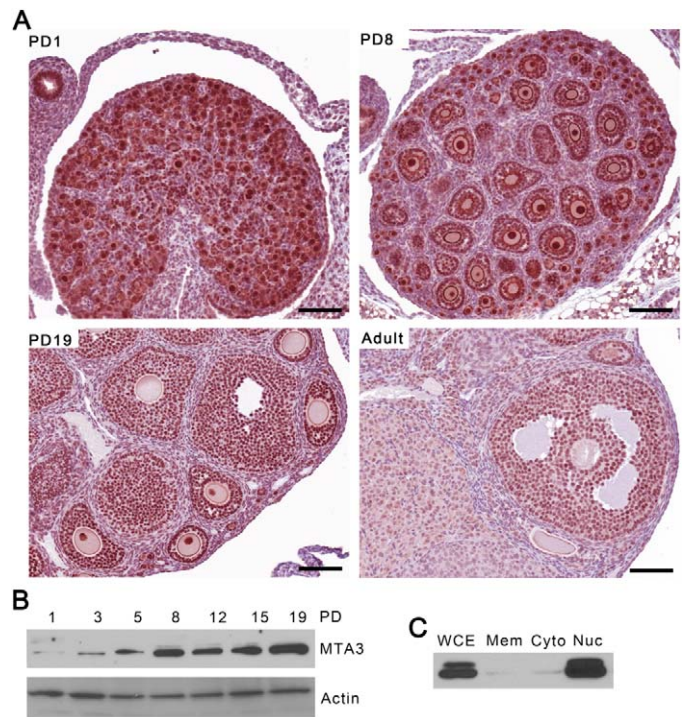


FIG. 1. Expression and cellular localization of MTA3 during follicle development. **A**) Ovary sections from the indicated Postnatal Day (PD) immunostained for MTA3 (brown). Bar = 100 μ m. **B**) Immunoblot of MTA3 (upper panel) in whole-ovary protein extracts collected on PDs 1, 3, 5, 8, 12, 15, and 19. Actin (lower panel) was used as a loading control. **C**) Immunoblot of MTA3 in fractionated granulosa cells extracts. WCE, whole-cell extract; Mem, membrane; Cyto, cytosolic; Nuc, nuclear.

suggesting the possibility of a posttranslational modification. This second band remained even after the protein extracts were treated with phosphatase, indicating that it was not a result of MTA3 phosphorylation (data not shown).

Initial computational analysis using the UCSC genome browser revealed four major MTA3 splice variants that encode proteins composed of 513–591 amino acids (Fig. 2A). In addition, one reported MTA3 transcript differed from variant 1 by insertion of three nucleotides encoding a serine residue. This variant, which we referred to as variant 1A (accession number uc008dsf.1), can be explained by usage of an alternative splice site three nucleotides upstream of the exon 12 splice junction used by variant 1B (accession number uc008dsg.1) (Fig. 2A). Of note, all four MTA3 isoforms retain the highly conserved protein-protein interaction domains typical of the MTA3 family, including histone interaction, GATA-like zinc finger, and DNA-binding domains, suggesting that all are capable of serving within protein complexes interacting with chromatin.

To determine which of these MTA3 forms were expressed in granulosa cells, RT-PCR was used. Granulosa cell cDNA encoding three regions of MTA3 was amplified: exons 2–7, exons 7–12, and exon 12 through a 3' untranslated region (3'-UTR) that was unique for each variant (Fig. 2A). All variants were present in mouse granulosa cells (Fig. 2B), although variant 1 appeared to be the most abundantly expressed based on the intensity of the amplified band. The PCR products were sequenced to confirm their identity, revealing that all four variants sometimes included the three-nucleotide insertion. To determine the relative expression of the two subtypes (A and B) in granulosa cells, we designed fluorescent TaqMan PCR probes to differentiate between the variants. In granulosa cells

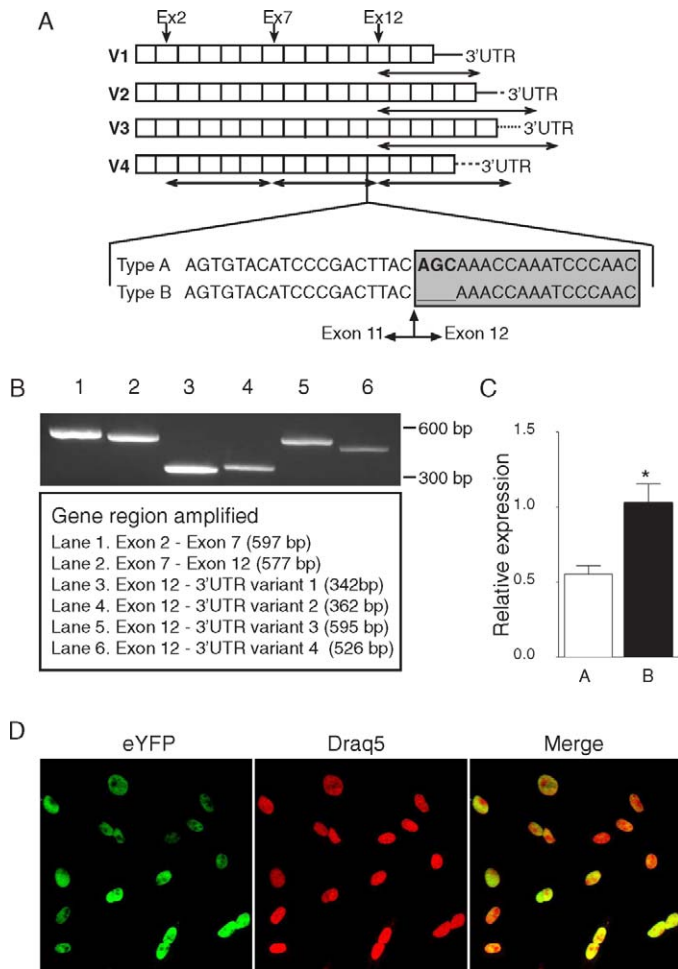


FIG. 2. Expression and localization of MTA3 splice variants. **A)** Schematic of four MTA3 splice variants present in mouse granulosa cells. GenBank accession numbers of splice variants: V1, uc008dsf.1; V2, uc008dsh.1; V3, uc008dsi.1; and V4, uc008dsj.1. White boxes indicate individual exons. Horizontal bidirectional arrows indicate amplified regions between exons 2, 7, and 12 and unique 3'-UTRs. Position of the three-nucleotide insertion between exons 11 and 12 is shown. **B)** Agarose gel showing PCR analysis of MTA3 splice variants along with lane description, including PCR product size in base pair (bp). **C)** TaqMan PCR analysis demonstrating relative expression of type A vs. type B variants of MTA3 in Postnatal Day 20 mouse ovary. * $P < 0.05$, Mann-Whitney U -test. **D)** Cellular localization of MTA variant 1 type A in granulosa cells infected with lentivirus encoding MTA3-EYFP. Left panel, MTA3-EYFP (green); middle panel, DNA (red); right panel, merged image.

isolated from Postnatal Day 20 ovaries, expression of subtype B (not containing the serine residue) was approximately twice that of subtype A (Fig. 2C). This subtype B:subtype A ratio was consistently observed in cDNA isolated from ovaries at all stages of postnatal development and from adult ovaries after gonadotropin stimulation (data not shown). To determine if the subtype A serine residue affected protein localization, EYFP-tagged forms of MTA3 variants 1A and 1B were expressed in granulosa cells. Both variants localized only to the nuclei; localization of variant 1A is shown in Figure 2D.

MTA3 Interaction with NuRD and Cohesin Complexes in the Ovary

It has been suggested that members of the MTA family are mutually exclusive within the NuRD complex [5, 13]. To date,

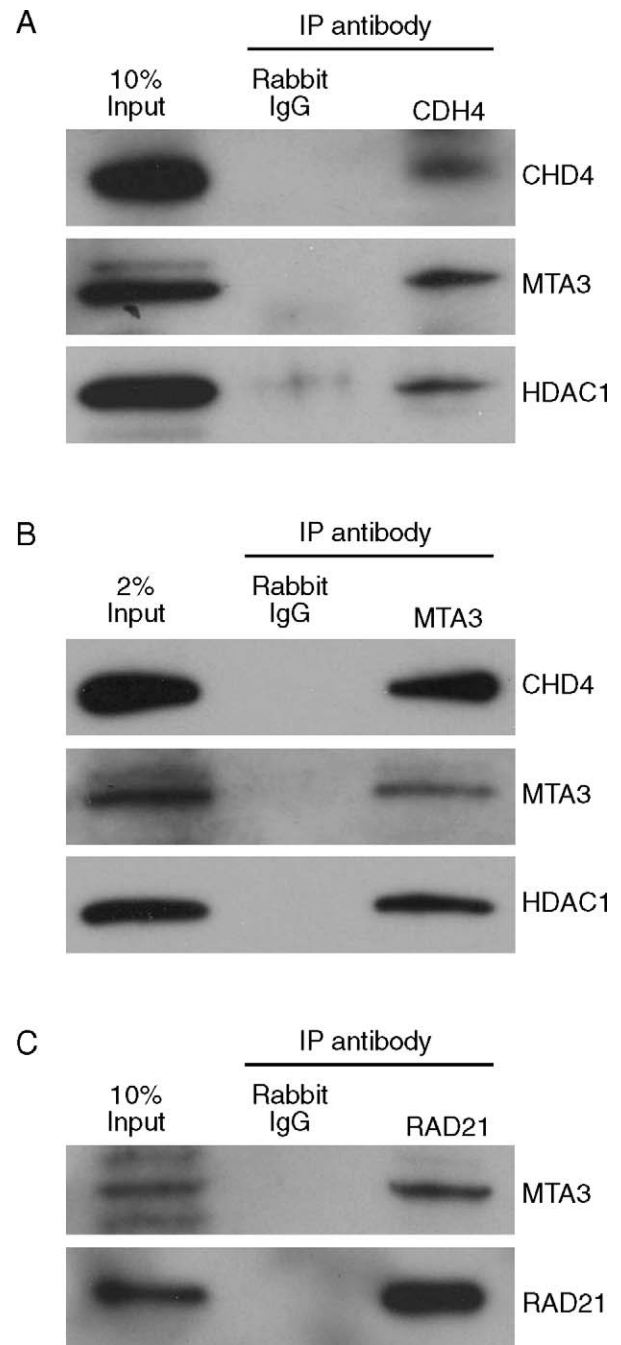


FIG. 3. Immunoprecipitation of MTA3 with NuRD and cohesin complex proteins. Immunoblots of ovary extracts immunoprecipitated using CHD4 (A), MTA3 (B), or RAD21 (C) antibodies. Nonimmune rabbit IgG was used as a negative control for all immunoprecipitations. Antibodies used for immunoblots are indicated on the right. In all panels, input protein extract (% indicated) served as a positive control.

all three members of the MTA family have been found to be NuRD subunits in different cell types [25, 29–31]. To determine whether MTA3 is a component of the NuRD complex in ovaries in vivo, we performed coimmunoprecipitation experiments using antibodies specific for two major subunits of the NuRD complex, CHD4 and HDAC1.

Immunoprecipitation of CHD4 from whole-ovary extracts resulted in coprecipitation of both MTA3 and HDAC1 (Fig. 3A). The reciprocal was also true (i.e., immunoprecipitation of MTA3 resulted in coprecipitation of CHD4 and HDAC1) (Fig.

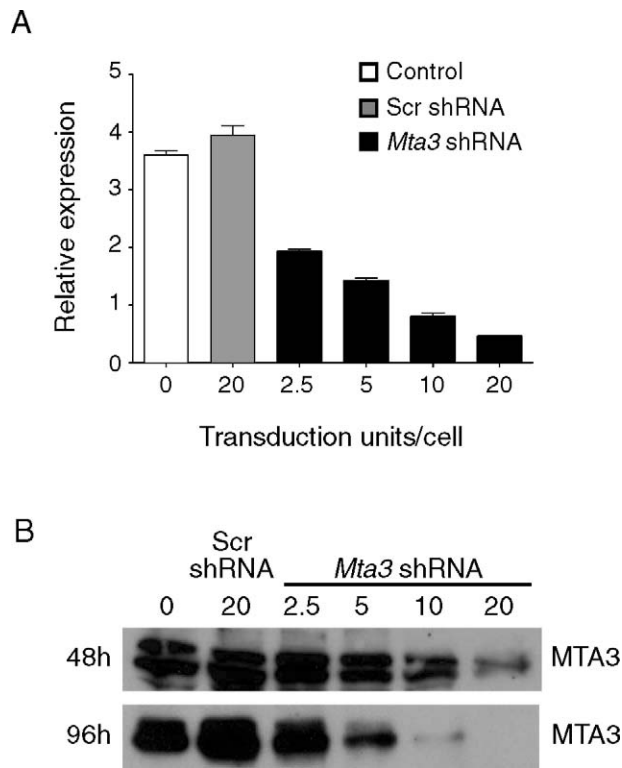


FIG. 4. Efficacy of MTA3 knockdown in primary granulosa cells. **A**) Real-time RT-PCR analysis showing relative expression of MTA3 96 h after infection with the indicated number of transduction units per cell. Control, no lentivirus (white bars); Scr, scrambled (gray bars); MTA3 (black bars). **B**) Immunoblots of MTA3 48 h (upper panel) and 96 h (lower panel) after infection; TU/cell are indicated above each lane.

3B). These findings indicate that MTA3 interacts with NuRD complex proteins *in vivo*. Because the NuRD complex participates in cohesin loading onto chromosomes in HeLa cells [18], we tested whether MTA3 interacts with RAD21, a major cohesin complex protein. RAD21 coimmunoprecipitated with MTA3 (Fig. 3C), indicating that these two proteins also interact in ovarian cells *in vivo*.

MTA3 Function in Granulosa Cells *In Vitro*

To determine the function of MTA3, we knocked down MTA3 in primary mouse granulosa cells proliferating *in vitro*. Granulosa cells were infected with a lentiviral construct encoding an shRNA targeting a region of *Mta3* conserved in all variant forms. Uninfected granulosa cells or cells infected with a scrambled shRNA sequence were used as controls. A dose-dependent decrease in *Mta3* mRNA was observed 96 h after infection only in *Mta3* shRNA-treated cells (Fig. 4A). Twenty TU/cell of *Mta3* shRNA resulted in a 95% decrease in *Mta3* mRNA 96 h after infection compared with control cells infected with the scrambled shRNA sequence. MTA3 protein was partially reduced 48 h after infection with both 10 and 20 TU/cell of *Mta3* shRNA and was not detected at all 96 h after infection with 20 TU/cell (Fig. 4B). No change in MTA3 protein was observed in control cells at either time point.

Treatment of proliferating granulosa cells with *Mta3* shRNA resulted in an apparent loss of confluence compared with controls, suggesting that the cells were proliferating more slowly or that cell death was occurring. Cell proliferation over time after infection was measured using a metabolic assay. Control cells treated with scrambled shRNA proliferated at a

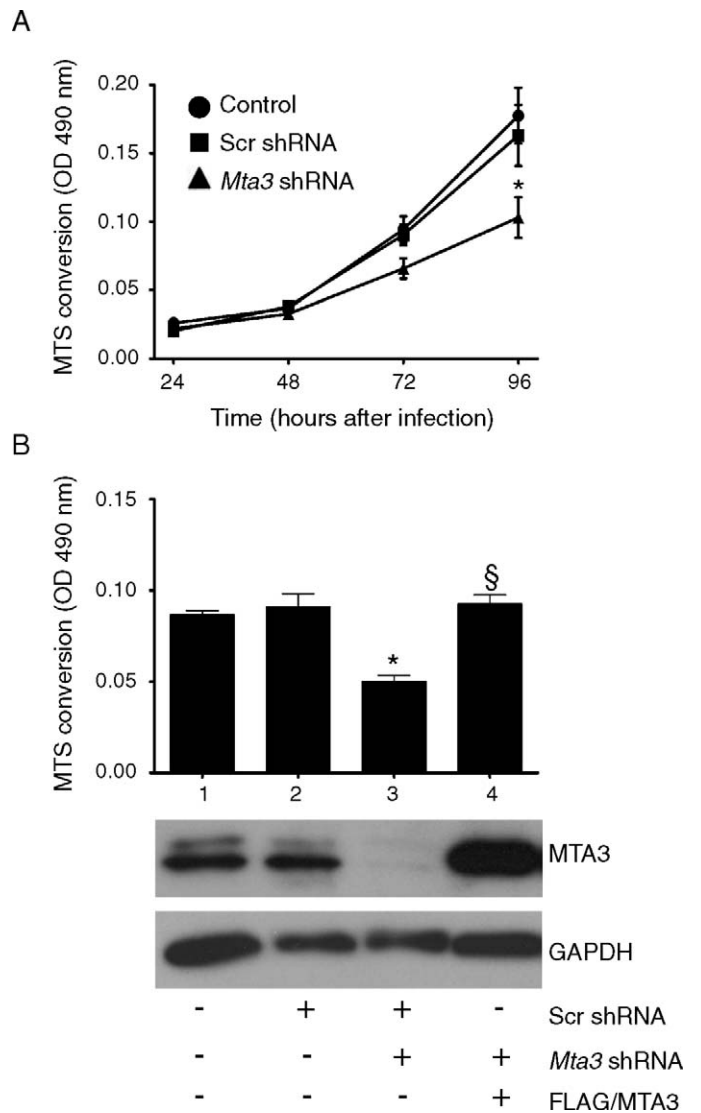


FIG. 5. Effect of MTA3 depletion on cell proliferation. **A**) Granulosa cells were cultured 24–96 h after infection with no lentivirus (Control) or 20 TU/cell of lentiviral particles containing scrambled (Scr) shRNA or *Mta3* shRNA. The readout of the MTS metabolic assay is shown on the y-axis. * $P < 0.001$ vs. control and scrambled shRNA. Two-way ANOVA, followed by Bonferroni post hoc test, was used. **B**) Rescue of granulosa cell proliferation. Granulosa cells were cultured 96 h after infection with 1) no lentivirus or (2–4) a total of 22 TU/cell of lentiviral particles as follows: 2) Scrambled shRNA, 22 TU/cell; 3) *Mta3* shRNA, 20 TU/cell, plus scrambled shRNA, 2 TU/cell; or 4) *Mta3* shRNA, 20 TU/cell, plus MTA3 variant 1 type A 2 TU/cell. The graph indicates the readout of the MTS metabolic assay. Shown below the graph are representative immunoblots of cell extracts collected after MTS assay. Blots were probed using MTA3 and GAPDH antibodies as indicated. * $P < 0.001$ vs. control and scrambled shRNA; [§] $P < 0.01$ vs. *Mta3* shRNA. One-way ANOVA, followed by Tukey post hoc test, was used.

rate similar to uninfected cells, increasing their number almost eight-fold over 96 h (Fig. 5A). MTA3-depleted cells proliferated but not as rapidly as controls, such that by 96 h after infection their number was 40% lower than the scrambled shRNA-treated cells. To determine whether the inhibitory effects of *Mta3* shRNA on cell proliferation were due specifically to loss of MTA3 protein, we coinfecting the cells with a lentiviral expression vector encoding MTA3 variant 1A mutated in the region targeted by *Mta3* shRNA but encoding an amino acid sequence identical to the wild-type variant.

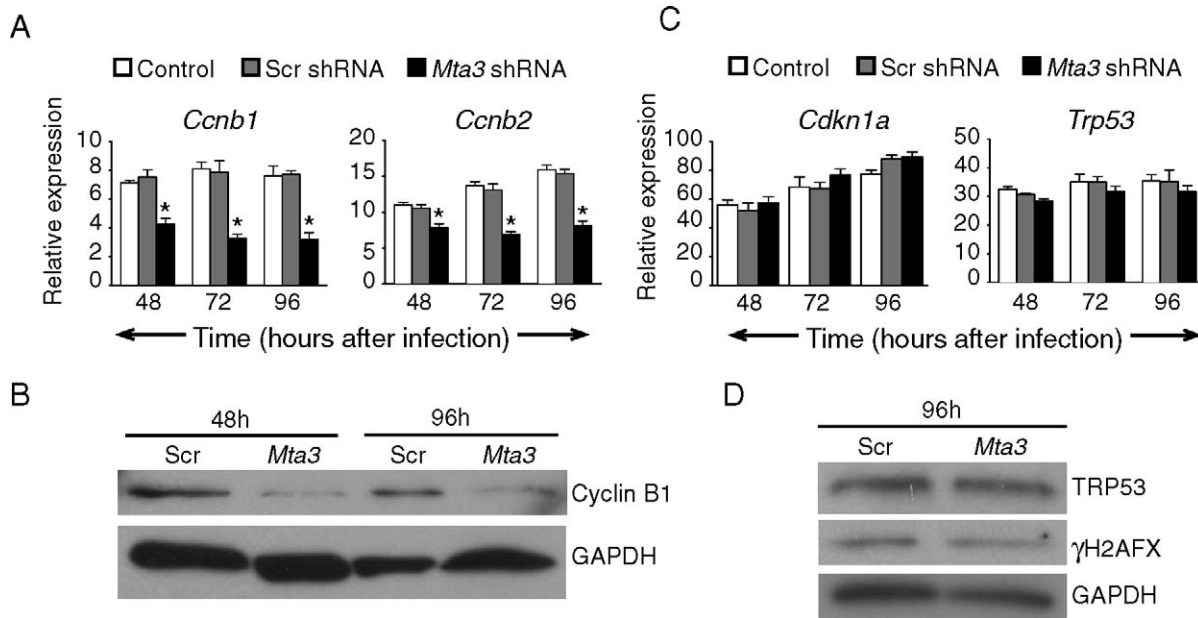


FIG. 6. Effects of MTA3 depletion on cell cycle proteins. **A**) Relative expression of *Ccnb1* and *Ccnb2* mRNA over time after infection with the indicated lentivirus construct. * $P < 0.01$ vs. scrambled (Scr) shRNA. Two-way ANOVA, followed by Bonferroni post hoc test, was used. **B**) Immunoblot of cyclin B1 protein at 48 and 96 h after lentiviral infection with scrambled or *Mta3* shRNA as indicated. **C**) Relative expression of *Cdkn1a* and *Trp53* mRNA over time after infection with the indicated lentivirus construct. **D**) Immunoblots of TRP53 and γ H2AFX 96 h after lentiviral infection with scrambled or *Mta3* shRNA as indicated. GAPDH was used as a loading control for all immunoblots.

Granulosa cells treated concomitantly with *Mta3* shRNA and lentivirus encoding exogenous MTA3 variant 1A proliferated normally, suggesting that inhibition of cell proliferation was a specific result of MTA3 protein depletion (Fig. 5B). Similar results were observed when MTA3 variant 1B was coexpressed with the *Mta3* shRNA (data not shown). These rescue experiments suggested that cells lacking MTA3 do not undergo apoptosis but rather that the inhibitory effect on proliferation was caused by slowing of the cell cycle or induction of earlier quiescence in culture.

To determine whether loss of MTA3 was associated with specific alterations in the cell cycle, we compared the expression of various cyclins in the treated cells vs. controls. There was a decrease in mRNA encoding both cyclin B1 and cyclin B2 by 48 h after *Mta3* shRNA treatment was initiated (Fig. 6A). This finding was confirmed at the protein level for cyclin B1 (Fig. 6B). Expression of cyclins A1, D1, D2, E1, and G1 was no different between treatment groups (data not shown). Interestingly, downregulation of cyclin B1 and cyclin B2 expression preceded the inhibitory effects on cell proliferation, suggesting that joint action of MTA3 and cyclin B is required during preparation for mitosis.

It was previously shown that inhibitory effects on cell proliferation similar to those we induced by MTA3 depletion can also be induced by depletion of CHD4, the major NuRD complex subunit, in immortalized human osteosarcoma U2OS cells [22]. In that study, slowing of proliferation was apparently a result of accumulation of spontaneous DNA damage characterized by increased phosphorylation of histone γ H2AFX, changes in *CDKN1A* (previously *p21*) and *TP53* (previously *p53* [human homolog of mouse *Trp53*]) expression, and activation of the G0/S checkpoint. To determine if a similar mechanism explained our findings, we examined expression of *Cdkn1a* and *Trp53* in MTA3-depleted granulosa cells. Expression of *Cdkn1a* and *Trp53* mRNA was no different in MTA3-depleted cells compared with controls (Fig. 6C). Because TRP53 protein is typically regulated by

ubiquitin-mediated protein degradation, the level of TRP53 was also examined by immunoblotting. We found that TRP53 protein was unchanged; moreover, phosphorylation of γ H2AFX was unaffected by MTA3 knockdown (Fig. 6D).

We next examined whether there was any alteration in the percentage of cells in the various stages of the cell cycle in MTA3-depleted cells compared with controls. Flow cytometry experiments revealed that cell populations lacking MTA3 contained a significantly higher percentage of cells in G2/M phase and a lower percentage of cells in S phase compared with controls (Fig. 7A). There was no measurable sub-G1 fraction in either treatment group, indicating a lack of apoptotic cells. Because the G2/M transition appeared to be slowed, we examined phosphorylation of histone H3 at serine 10 (H3Ser10), a marker of a successful G2/M shift. Phosphorylation of histone H3 at this epitope was significantly reduced (Fig. 7B), suggesting that reduction in MTA3 affects the G2/M transition of cells and results in delayed entry into mitosis.

DISCUSSION

In the present study, we characterized MTA3 in the mouse ovary and examined its function in primary mouse granulosa cells. MTA3 not only interacts with NuRD complex proteins, as expected, but also coprecipitates with the major cohesin complex subunit RAD21. MTA3 protein knockdown in primary granulosa cells results in slowing of cell proliferation associated with reductions in cyclin B1 and cyclin B2 expression and a delay in the G2/M cell cycle transition. These findings demonstrate that MTA3 is a NuRD complex constituent that can interact with the cohesin complex in the ovary and suggest that the MTA3-NuRD complex functions with the cohesin complex to support cell cycle progression and growth of the granulosa cell compartment during follicle development *in vivo*.

Based on coprecipitation with CHD4 and HDAC1, at least some of the NuRD complex in the ovary contains MTA3.

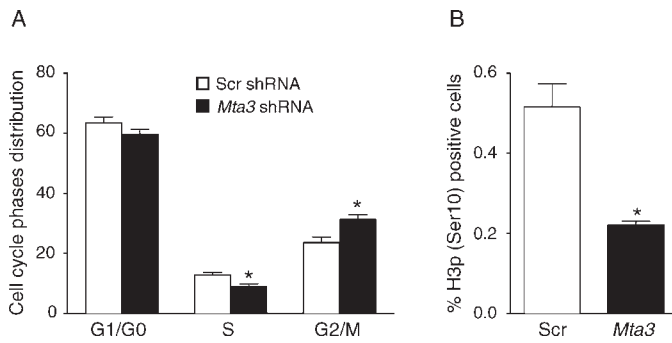


FIG. 7. Effect of MTA3 depletion on cell cycle distribution and histone H3 phosphorylation. Granulosa cells were infected with lentiviral particles containing 20 TU/cell of scrambled (Scr) or *Mta3* shRNA. **A**) Percentage of total cells in G1/G0, S, and G2/M phases. **B**) Simultaneous analysis of the same cells for histone H3 phosphorylation at serine 10. * $P < 0.05$. Two-way ANOVA, followed by Bonferroni post hoc test (A) or Mann-Whitney *U*-test (B), was used.

Although this does not exclude the possibility that MTA3 could act in association with other complexes or alone, it is likely that the slowing of cell proliferation is caused by alterations in NuRD complex function that result from a lack of MTA3. Indeed, knockdown of MBD3, a subunit required for NuRD integrity and stability, delays the G2/M transition and is associated with downregulation of cyclin B1 in several cancer cell lines [32]. Similar delays in the G2/M transition associated with reduced cyclin B1 expression are observed following chemical and functional inhibition of HDAC1 [33]. These observations suggest that MTA3 is required to support effective chromatin-remodeling activity of the NuRD complex in granulosa cells.

Cells duplicate their DNA content during S phase, and toward the end of this phase, newly synthesized sister chromatids are held together by the cohesin complex, particularly in pericentromeric regions, to facilitate faithful chromosome segregation during M phase [34]. In human cell lines, association of the cohesin complex with chromatin is facilitated by both ISWI and NuRD chromatin-remodeling complexes through their SMARCA5 and CHD4 subunits, respectively, which interact directly with the core cohesin component RAD21 [18]. Interestingly, NuRD associates with pericentromeric heterochromatin during late S phase in rapidly proliferating lymphoid cell lines and in primary germinal center B cells, suggesting that it facilitates cohesin loading in lymphoid cells [35]. In the present study, we show that, similar to the ISWI complex subunit SMARCA5 [36], MTA3 expression is significantly lower in terminally differentiated nondividing corpus luteum cells than in ovarian granulosa cells. These findings, combined with the observation that MTA3 depletion slows granulosa cell proliferation by affecting the G2/M transition, suggest that both the ISWI and NuRD complexes function to facilitate cohesin loading and sister chromatid stabilization during mitosis in granulosa cells.

The NuRD components MTA1, MTA2, and CHD4 facilitate DNA double-strand break repair [17], and this effect could be mediated by modulation of cohesin association with repair foci. It is unlikely that MTA3 depletion in granulosa cells resulted in slowing of cell proliferation due to accumulation of DNA double-strand breaks. This statement is based on our findings that MTA3 depletion did not affect *Cdkn1a* or *Trp53* expression, TRP53 protein levels, or γ H2AFX phosphorylation. Instead, slowing of the transition through the G2/M checkpoint due to inhibition of cyclin B

expression or slower cohesin complex loading in the absence of MTA3 is a more likely explanation.

The concerted activity of several kinases is required for mitotic entry to occur with normal timing. One such kinase, aurora B, phosphorylates H3Ser10 in pericentromeric chromatin regions beginning in late G2 phase [37]. This phosphorylation mark spreads along the chromosomes as mitosis proceeds and is complete in prophase; thus, it can serve as a mark of G2/M progression [38]. In the rat, H3Ser10 phosphorylation is most prominent during proestrus in granulosa cells of growing follicles [39], confirming an association of this mark with estrogen-mediated proliferation of primary granulosa cells. In mouse primary granulosa cell cultures, we found that MTA3 depletion caused more than a two-fold decrease in cells positive for H3Ser10 phosphorylation; however, less than 1% of cells in either treatment group exhibited this mark. The low incidence of H3Ser10 phosphorylation in both groups is consistent with the relatively slow cell proliferation we observed in these primary cells cultured in the absence of mitogenic stimuli like follicle-stimulating hormone or estradiol.

Later stages of chromosome condensation rely on the master mitotic complex cyclin-B1-CDK1, which triggers mitotic entry by initiating nuclear envelope breakdown [40]. At this point, cells become committed to mitosis and proceed into prometaphase, even if stressed [41]. Expression of type B cyclins in normally proliferating animal cells begins to rise in late S phase, reaches a maximum in the middle of G2/M phase, and drops immediately upon completion of mitosis [42]. Transcription of cyclin B1 and cyclin B2 is regulated by transcriptional activators and repressors that bind promoter elements common to many cell cycle genes [43]. We found that expression of cyclin B1 and cyclin B2 is significantly reduced following MTA3 knockdown. One explanation for this finding is that MTA3 serves directly as a transcriptional activator or coactivator. There are precedents for MTA proteins serving in this role because MTA1 stimulates PAX5 transcription in B cells by a direct interaction with its promoter and interacts with the transactivator HBx to promote nitric oxide synthase 2 transcription in hepatocellular carcinoma cells [44, 45]. A direct role for MTA3 in regulating cyclin B expression via promoter interactions is possible even though there is no evidence published to date that MTA3 serves as a transcriptional activator. However, it was recently shown that the cohesin complex can function to modulate chromatin architecture in ways that stabilize enhancer-promoter interactions important for gene transcription [19]. This observation raises the possibility that MTA3 and/or the MTA3-NuRD complex supports cohesin-chromatin interactions required to promote sufficient cyclin B expression to transit the G2/M checkpoint.

Taken together, our studies indicate that MTA3 is a NuRD complex subunit in granulosa cells and support the idea that the MTA3-NuRD complex functions to support chromatin remodeling required for cohesin loading and G2/M progression. These findings highlight the critical role of the NuRD chromatin-remodeling complex in cell cycle control, in addition to its well-documented functions in modulating epigenetic marks that control gene transcription and in DNA double-strand break repair.

ACKNOWLEDGMENT

We thank Gary Powell, Negin Martin, Carl Bortner, and Maria Sifre (NIEHS) for technical support; Grace Kissling (NIEHS) for help with statistical analysis; and Dominic Esposito (National Cancer Institute, National Institutes of Health) for providing the viral expression vector pDest-673.

REFERENCES

1. Fortune JE. Ovarian follicular growth and development in mammals. *Biol Reprod* 1994; 50:225–232.
2. Richards JS. Hormonal control of gene expression in the ovary. *Endocr Rev* 1994; 15:725–751.
3. Richards JS. Perspective: the ovarian follicle: a perspective in 2001. *Endocrinology* 2001; 142:2184–2193.
4. Lavoie HA, King SR. Transcriptional regulation of steroidogenic genes: STARD1, CYP11A1 and HSD3B. *Exp Biol Med (Maywood)* 2009; 234:880–907.
5. Ho L, Crabtree GR. Chromatin remodelling during development. *Nature* 2010; 463:474–484.
6. Bannister AJ, Kouzarides T. The CBP co-activator is a histone acetyltransferase. *Nature* 1996; 384:641–643.
7. Ogrzyzko VV, Schiltz RL, Russanova V, Howard BH, Nakatani Y. The transcriptional coactivators p300 and CBP are histone acetyltransferases. *Cell* 1996; 87:953–959.
8. LaVoie HA. Epigenetic control of ovarian function: the emerging role of histone modifications. *Mol Cell Endocrinol* 2005; 243:12–18.
9. Sengupta N, Seto E. Regulation of histone deacetylase activities. *J Cell Biochem* 2004; 93:57–67.
10. Lazzaro MA, Pepin D, Pescador N, Murphy BD, Vanderhyden BC, Picketts DJ. The imitation switch protein SNF2L regulates steroidogenic acute regulatory protein expression during terminal differentiation of ovarian granulosa cells. *Mol Endocrinol* 2006; 20:2406–2417.
11. Nimz M, Spitschak M, Furbass R, Vanselow J. The pre-ovulatory luteinizing hormone surge is followed by down-regulation of CYP19A1, HSD3B1, and CYP17A1 and chromatin condensation of the corresponding promoters in bovine follicles. *Mol Reprod Dev* 2010; 77:1040–1048.
12. Hiroi H, Christenson LK, Chang L, Sammel MD, Berger SL, Strauss JF III. Temporal and spatial changes in transcription factor binding and histone modifications at the steroidogenic acute regulatory protein (stAR) locus associated with stAR transcription. *Mol Endocrinol* 2004; 18:791–806.
13. Bowen NJ, Fujita N, Kajita M, Wade PA. Mi-2/NuRD: multiple complexes for many purposes. *Biochim Biophys Acta* 2004; 1677:52–57.
14. Denslow SA, Wade PA. The human Mi-2/NuRD complex and gene regulation. *Oncogene* 2007; 26:5433–5438.
15. Eisen JA, Sweder KS, Hanawalt PC. Evolution of the SNF2 family of proteins: subfamilies with distinct sequences and functions. *Nucleic Acids Res* 1995; 23:2715–2723.
16. Woodage T, Basrai MA, Baxeivanis AD, Hieter P, Collins FS. Characterization of the CHD family of proteins. *Proc Natl Acad Sci U S A* 1997; 94:11472–11477.
17. Tong JK, Hassig CA, Schnitzler GR, Kingston RE, Schreiber SL. Chromatin deacetylation by an ATP-dependent nucleosome remodelling complex. *Nature* 1998; 395:917–921.
18. Hakimi MA, Bochar DA, Schmiesing JA, Dong Y, Barak OG, Speicher DW, Yokomori K, Shiekhhattar R. A chromatin remodelling complex that loads cohesin onto human chromosomes. *Nature* 2002; 418:994–998.
19. Kagey MH, Newman JJ, Bilodeau S, Zhan Y, Orlando DA, van Berkum NL, Ebmeier CC, Goossens J, Rahl PB, Levine SS, Taatjes DJ, Dekker J, et al. Mediator and cohesin connect gene expression and chromatin architecture. *Nature* 2010; 467:430–435.
20. Polo SE, Kaidi A, Baskcomb L, Galanty Y, Jackson SP. Regulation of DNA-damage responses and cell-cycle progression by the chromatin remodelling factor CHD4. *EMBO J* 2010; 29:3130–3139.
21. Chou DM, Adamson B, Dephoure NE, Tan X, Nottke AC, Hurov KE, Gygi SP, Colaiacovo MP, Elledge SJ. A chromatin localization screen reveals poly (ADP ribose)-regulated recruitment of the repressive polycomb and NuRD complexes to sites of DNA damage. *Proc Natl Acad Sci U S A* 2010; 107:18475–18480.
22. Smeenk G, Wiegant WW, Vrolijk H, Solari AP, Pastink A, van Attikum H. The NuRD chromatin-remodeling complex regulates signaling and repair of DNA damage. *J Cell Biol* 2010; 190:741–749.
23. Larsen DH, Poinsignon C, Gudjonsson T, Dinant C, Payne MR, Hari FJ, Danielsen JM, Menard P, Sand JC, Stucki M, Lukas C, Bartek J, et al. The chromatin-remodeling factor CHD4 coordinates signaling and repair after DNA damage. *J Cell Biol* 2010; 190:731–740.
24. Li DQ, Pakala SB, Reddy SD, Ohshiro K, Peng SH, Lian Y, Fu SW, Kumar R. Revelation of p53-independent function of MTA1 in DNA damage response via modulation of the p21 WAF1-proliferating cell nuclear antigen pathway. *J Biol Chem* 2010; 285:10044–10052.
25. Fujita N, Jaye DL, Kajita M, Geigerman C, Moreno CS, Wade PA. MTA3, a Mi-2/NuRD complex subunit, regulates an invasive growth pathway in breast cancer. *Cell* 2003; 113:207–219.
26. Fujita N, Kajita M, Taysavang P, Wade PA. Hormonal regulation of metastasis-associated protein 3 transcription in breast cancer cells. *Mol Endocrinol* 2004; 18:2937–2949.
27. Pfaffl MW. A new mathematical model for relative quantification in real-time RT-PCR. *Nucleic Acids Res* 2001; 29:
28. Salmon P, Trono D. Production and titration of lentiviral vectors. *Curr Protoc Neurosci* 2006; Chapter 4:Unit 4.21.
29. Fujita N, Jaye DL, Geigerman C, Akyildiz A, Mooney MR, Boss JM, Wade PA. MTA3 and the Mi-2/NuRD complex regulate cell fate during B lymphocyte differentiation. *Cell* 2004; 119:75–86.
30. Xue Y, Wong J, Moreno GT, Young MK, Cote J, Wang W. NURD: a novel complex with both ATP-dependent chromatin-remodeling and histone deacetylase activities. *Mol Cell* 1998; 2:851–861.
31. Yao YL, Yang WM. The metastasis-associated proteins 1 and 2 form distinct protein complexes with histone deacetylase activity. *J Biol Chem* 2003; 278:42560–42568.
32. Noh EJ, Lim DS, Lee JS. A novel role for methyl CpG-binding domain protein 3, a component of the histone deacetylase complex, in regulation of cell cycle progression and cell death. *Biochem Biophys Res Commun* 2009; 378:332–337.
33. Noh EJ, Lee JS. Functional interplay between modulation of histone deacetylase activity and its regulatory role in G2-M transition. *Biochem Biophys Res Commun* 2003; 310:267–273.
34. Xiong B, Gerton JL. Regulators of the cohesin network. *Annu Rev Biochem* 2010; 79:131–153.
35. Helbling Chadwick L, Chadwick BP, Jaye DL, Wade PA. The Mi-2/NuRD complex associates with pericentromeric heterochromatin during S phase in rapidly proliferating lymphoid cells. *Chromosoma* 2009; 118:445–457.
36. Lazzaro MA, Picketts DJ. Cloning and characterization of the murine Imitation Switch (ISWI) genes: differential expression patterns suggest distinct developmental roles for Snf2h and Snf2l. *J Neurochem* 2001; 77:1145–1156.
37. Becker M, Stolz A, Ertych N, Bastians H. Centromere localization of INCENP-aurora B is sufficient to support spindle checkpoint function. *Cell Cycle* 2010; 9:1360–1372.
38. Prigent C, Dimitrov S. Phosphorylation of serine 10 in histone H3: what for? *J Cell Sci* 2003; 116:3677–3685.
39. Ruiz-Cortes ZT, Kimmins S, Monaco L, Burns KH, Sassone-Corsi P, Murphy BD. Estrogen mediates phosphorylation of histone H3 in ovarian follicle and mammary epithelial tumor cells via the mitotic kinase, Aurora B. *Mol Endocrinol* 2005; 19:2991–3000.
40. Barr AR, Gergely F. Aurora-A: the maker and breaker of spindle poles. *J Cell Sci* 2007; 120:2987–2996.
41. Pines J, Rieder CL. Re-staging mitosis: a contemporary view of mitotic progression. *Nat Cell Biol* 2001; 3:E3–E6.
42. Ito M. Factors controlling cyclin B expression. *Plant Mol Biol* 2000; 43:677–690.
43. Fung TK, Poon RY. A roller coaster ride with the mitotic cyclins. *Semin Cell Dev Biol* 2005; 16:335–342.
44. Balasenthil S, Gururaj AE, Talukder AH, Bagheri-Yarmand R, Arrington T, Haas BJ, Braisted JC, Kim I, Lee NH, Kumar R. Identification of Pax5 as a target of MTA1 in B-cell lymphomas. *Cancer Res* 2007; 67:7132–7138.
45. Bui-Nguyen TM, Pakala SB, Sirigiri DR, Martin E, Murad F, Kumar R. Stimulation of inducible nitric oxide by hepatitis B virus transactivator protein HBx requires MTA1 coregulator. *J Biol Chem* 2010; 285:6980–6986.